Available online at www.sciencedirect.com
ScienceDirect
Journal of Nuclear Materials 359 (2006) 80–92
journal of nuclear materials
www.elsevier.com/locate/jnucmat

Effect of feed solution composition and heat treatment conditions on the morphology of uranium oxide microspheres prepared by sol–gel process

N. Kumar [a], Y.R. Bamankar [a], K.T. Pillai [a], S.K. Mukerjee [a,*], V.N. Vaidya [b], V. Venugopal [c]

[a] *Fuel Chemistry Division, Bhabha Atomic Research Centre, Mumbai 400085, India*
[b] *DAE, BRNS, Mumbai 400085, India*
[c] *Radiochemistry and Isotope Group, Bhabha Atomic Research Centre, Mumbai 400085, India*

Received 13 January 2006; accepted 30 July 2006

Abstract

Uranium oxide microspheres were prepared by internal gelation process (IGP) using selected feed solution compositions. In the feed, concentration of uranium was maintained at 1.25 M and hexamethylenetetramine (HMTA)-urea to uranium mole ratio (R) was varied between 1.2 and 1.5. The gel particles obtained from each batch were heated at 250 °C in air. The samples from each batch were heated under various heat treatment conditions, such as calcination to U_3O_8, reduction of calcined U_3O_8 and direct reduction of UO_3 to UO_2. The effect of feed solution composition and heat treatment conditions on the morphology of the uranium oxide microspheres was studied by measuring surface area, pore size distribution, pore volume, tap density and crush strength. The details of open and closed pores on the dried and heat treated products were studied by scanning electron microscope (SEM) analysis.

PACS: 68.55.Jk; 68.37.Hk; 68.43.Mn

1. Introduction

Uranium oxide microspheres prepared by internal gelation process (IGP) [1,2] could be used either for the fabrication of UO_2 pellets by sol–gel microsphere pelletization technique (SGMP) [3–5] or for the fabrication of sphere-pac fuel pins [6] using high-density microspheres. The composition of the feed and the conditions of heat treatment dictate the quality of the resulting UO_2 microspheres. It is therefore essential to carry out a systematic study on the nature of UO_2 microspheres obtained using different feed solution compositions and heated under various heat treatment conditions. The gel pelletization technique employs free flowing, dust-free sol–gel derived microspheres, in place of powders, as feed material for making pellets. This

* Corresponding author. Tel.: +91 22 25594578; fax: +91 22 25505345.
E-mail address: smukerji@magnum.barc.ernet.in (S.K. Mukerjee).

0022-3115/$ - see front matter © 2006 Elsevier B.V. All rights reserved.
doi:10.1016/j.jnucmat.2006.07.019

technique combines the advantageous front end flow sheet of the sol–gel process and the established rear end of the powder pelletization process. This process not only eliminates radiotoxic dust generating steps but also offers reproducible die fill for the fabrication of pellets due to the good flowability of the microspheres. Soft UO_2 microspheres could be obtained by the addition of carbon powder [7–12] during the preparation of UO_3 microspheres and its subsequent removal during calcination. Alternatively, soft UO_2 microspheres could also be obtained [13] by suitable selection of feed composition and introducing a calcination step to convert the dried UO_3 microspheres to U_3O_8 prior to its reduction to UO_2. The present investigation deals with understanding the effect of feed solution composition on the morphology of the microspheres. Efforts were also made to explain the role of introduction of calcination step prior to reduction, in imparting softness to the UO_2 microspheres.

2. Experimental

2.1. Chemicals

Nuclear grade uranium oxide powder was obtained from uranium metal plant, BARC. Uranyl nitrate solution was prepared by dissolving calculated amount of uranium oxide powder in analytical grade concentrated nitric acid. The calculated amounts of analytical grade hexamethylenetetramine (HMTA) and urea were dissolved in distilled water to obtain 3 M HMTA-urea solution.

2.2. Preparation of UO_3 microspheres

Uranium oxide microspheres were prepared by internal gelation process (IGP) [1,2]. Three batches were prepared; each with a batch volume of 200 ml using 0.8 mm internal diameter capillary. The compositions used were (i) $[U] = 1.25$ M and HMTA-urea/U mole ratio $(R) = 1.2$, (ii) $[U] = 1.25$ M and $R = 1.4$, and (iii) $[U] = 1.25$ M and $R = 1.5$. The compositions were selected from the opaque gel region of the gelation field diagram [2]. The gel particles obtained from each batch were washed first with carbon tetrachloride, and then with 5% ammonium hydroxide solution. The gel particles after completion of ammonia washing were transferred into a shallow silica boat and initially heated in an air oven at 100 °C for 8 h and then at 250 °C for 4 h to obtain dried microspheres of $UO_3 \cdot xNH_3\, yH_2O$ (where x and y are dependent on preparation conditions) [14,15].

2.3. Heat treatment of UO_3 microspheres

Around 5 g of the 250 °C heated sample (heating scheme A of Table 1) from each batch was taken for heat treatment studies. These samples were put in an alumina boat and heated in an electric resistance furnace. A programmable temperature controller was used to achieve a constant rate of heating. Samples from each batch were subjected to one of the four types of heat treatment methods shown below:

(A) direct reduction of UO_3 to UO_2 in $8\%H_2/92\%N_2$ gas at 600 °C for 1 h;
(B) direct reduction of UO_3 to UO_2 in $8\%H_2/92\%N_2$ gas at 800 °C for 1 h;
(C) calcination of UO_3 to convert to U_3O_8 in air at 800 °C for 1 h;
(D) calcination of UO_3 to convert to U_3O_8 in air at 800 °C for 1 h followed by reduction to UO_2 in $8\%H_2/92\%N_2$ gas at 600 °C for 1 h.

After reduction in $8\%H_2/92\%N_2$ gas mixture (containing impurities; oxygen = 4 vppm, moisture = 10 vppm, CO_2 and CO = 0.5 vppm, Ar = 10 vppm and hydrocarbon = 5 vppm) the microspheres were stabilized in CO_2 atmosphere to prevent their re-oxidation to U_3O_8 on exposure to air. The samples after each heat treatment were measured for surface area, pore size, pore volume, tap density and crush strength. The surface area of the samples was determined by multi-point BET method [16]. The adsorption–desorption isotherms and pore size distribution of the samples were determined by the static volumetric method using nitrogen gas adsorption–desorption techniques. The tap density was obtained by measuring the volume occupied by a known weight of the sample in a measuring cylinder after tapping. The crush strength was determined by measuring the load required for crushing a single microsphere in a crush strength measuring apparatus shown in Fig. 1.

2.4. Product characterization

2.4.1. Determination of surface area, pore volume and pore size

The surface area and pore size distribution were measured by a SORPTOMATIC 1990 analyser of

Table 1
Surface area, specific pore volume, tap density and crush strength of microspheres obtained from various feed compositions and heating conditions

No.	Feed composition[a], R	Heating scheme	Surface area (m^2/g)	Specific pore volume (cm^3/g)	Tap density (g/cm^3)	Crush strength (N/particle)
1	1.2	A	51.55	0.1079	1.52	9.2
2	1.4	A	54.91	0.0868	1.64	9.8
3	1.5	A	47.26	0.0962	1.62	10.5
4	1.2	B	17.26	0.0317	2.39	4.8
5	1.4	B	17.71	0.0280	2.63	6.8
6	1.5	B	15.84	0.0173	2.64	8.7
7	1.2	C	15.68	0.0166	2.54	6.3
8	1.4	C	13.14	0.0276	2.66	8.0
9	1.5	C	15.64	0.0307	2.69	8.9
10	1.2	D	6.75	0.0055	1.55	0.8
11	1.4	D	7.25	0.0085	1.62	1.0
12	1.5	D	5.69	0.0073	1.64	1.7
13	1.2	E	6.46	0.0051	2.13	2.9
14	1.4	E	5.45	0.0057	2.13	3.1
15	1.5	E	5.59	0.0059	2.18	3.1

A: UO_3 heated in air at 250 °C for 4 h.
B: Direct reduction of UO_3 to UO_2 in $8\%H_2/92\%N_2$ gas at 600 °C for 1 h.
C: Direct reduction of UO_3 to UO_2 in $8\%H_2/92\%N_2$ gas at 800 °C for 1 h.
D: Calcination of UO_3 to convert to U_3O_8 in air at 800 °C for 1 h.
E: Calcination of UO_3 to convert to U_3O_8 in air at 800 °C for 1 h followed by reduction to UO_2 in $8\%H_2/92\%N_2$ gas at 600 °C for 1 h.
[a] Uranium concentration: 1.25 M.

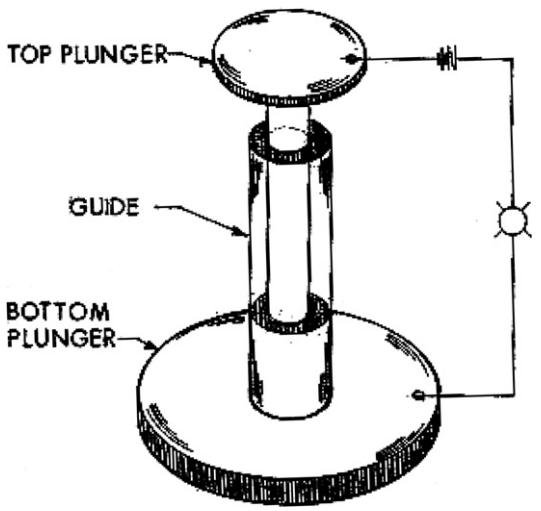

Fig. 1. Crush strength measuring apparatus.

CE Instruments, Italy. The microprocessor of this instrument receives the pre-treatment and analytical parameters from the personal computer (PC) and controls the injection pressure and volumes as a feed back of sample adsorption rate to optimise the number of equilibrium points to be collected. The data of equilibrium points, the injection parameters and saturation pressures are continuously transmitted to the PC for calculation. Software supplied by the manufacturer was used for calculations and obtaining graphs such as adsorption isotherms, pore size distribution pattern etc.

The specific surface area was measured by the multi-point BET method [16] using the lower pressure range of the adsorption isotherm, i.e. $0.05 \leqslant P/P_0 \leqslant 0.35$, where P is the equilibrium nitrogen pressure and P_0 is the saturation nitrogen pressure. On the other hand, the whole range of adsorption isotherm was used for pore analysis. To obtain the pore size distribution, the Kelvin equation [17] was used. The pore size distribution was calculated either by Barrett, Joyner and Halenda method (BJH method) [18] or by Horvath and Kawazoe method (HK method) [19].

2.4.2. Determination of tap density

For the measurement of tap density, the uranium oxide microspheres were taken in a 250 ml measuring cylinder and filled up to the mark. The cylinder was tapped for a fixed number of times in the vertical direction. The decrease in the volume of microspheres was adjusted by adding the corresponding amount of microspheres.

2.4.3. Determination of crush strength

The crush strength of the microspheres was determined by placing a single microsphere in the

groove of the lower plunger of a crush strength measuring apparatus shown in Fig. 1. The top plunger was carefully placed over the microsphere through a guide mechanism. The top and the bottom plungers were electrically connected so that a bulb lights when the two plungers contact by the break down of the microsphere. The weight required for crushing the microsphere (including the weight of the top plunger) gives the crush strength.

2.4.4. Pyconometric density measurement

The pyconometric density of the samples was determined by using a stereo pyconometer of Quanrachrome corporation USA. The instrument adopts the Archimedes principle of fluid displacement to determine the volume of the sample. The displaced fluid used was helium because it easily penetrates in the open pores of the microspheres giving high accuracies.

2.4.5. Microstructural examination by SEM

The gel particles prepared from the feed solution [U] = 1.25 M and $R = 1.2$ were heat treated as per the following heating schemes and used for porosity examinations using a Philips XL 30 scanning electron microscope, Netherlands:

(A) UO_3 heated in air at 250 °C for 4 h;
(B) direct reduction of UO_3 to UO_2 in 8%H_2/92%N_2 gas at 600 °C for 1 h;
(C) direct reduction of UO_3 to UO_2 in 8%H_2/92%N_2 gas at 800 °C for 1 h;
(D) calcination of UO_3 to convert to U_3O_8 in air at 800 °C for 1 h;
(E) calcination of UO_3 to convert to U_3O_8 in air at 800 °C for 1 h followed by reduction to UO_2 in 8%H_2/92%N_2 gas at 600 °C for 1 h.

SEM examinations was carried out for both the intact and fractured surfaces of the microspheres, which are considered to show the outer and inner surfaces, respectively. For them, the surface area and pore size analyses were also made.

3. Results and discussion

The first part deals with the effect of feed composition on the characteristics of the gel microspheres. The second part deals with the effect of different heat treatment schemes on the physical properties as related with the applicability to the SGMP process.

3.1. Effect of feed composition

The gel microspheres were prepared by varying a factor of the feed composition, R, from 1.2 to 1.5, keeping the metal concentration fixed at 1.25 M [20]. The surface area, specific pore volume, tap density and crush strength of the samples obtained by heating the gel microspheres, which are formed from the above feed compositions, with various heat treatment schemes are given in Table 1. It is seen from the table that the specific surface area, pore volume, tap density for 250 °C heated UO_3 microspheres (heating scheme A) do not show any systematic change with feed composition from $R = 1.2$ to 1.5. On the other hand, the pore size distribution is similar for all samples from $R = 1.2$ to 1.5, as can be estimated from the shape of the adsorption isotherms in the whole range of the P/P_0 ratio in Fig. 2. According to Brunaeur, Deming, Deming and Teller (BDDT) classifications, these isotherms can be placed under the category of type IV [21]. It can be seen from the adsorption curves that the 250 °C dried microspheres consists of pores covering the whole range of sizes from micro to macropores. The sharp increase in adsorption isotherm at higher partial pressure of nitrogen indicates the dominance of macro pores. Some information about the average pore size of the gel microspheres can be obtained from pore size distribution curves of the gel microspheres. The curves obtained by using the BJH method for the 250 °C heated sample and subsequently directly reduced sample at 600 °C are depicted in Figs. 3 and 4, respectively. Fig. 3 shows the pore size distribution curve, where Dv/Dr is the ratio of change in specific volume at two different partial pressures of nitrogen gas to difference in radius of pores at those pressures. It is seen that the average pore size in the 250 °C heated particles increases from about 100 Å for the gel particles prepared using high R (1.5) to 250 Å for the gel prepared from low R (1.2). As expected the pore size distribution of the directly reduced samples in Fig. 4 is shifted to higher size when compared with that of Fig. 3 as a result of product densification and pore merging. Variation of pore size with feed composition can be explained on the basis of chemistry of gelation [22]. Pai et al. [23] studied the effect of feed composition on the characteristics of ThO_2 and $(Th,U)O_2$ microspheres prepared by sol–gel process and suggested a procedure, based on the feed composition, for the preparation of soft gel particles suitable for SGMP. They concluded that

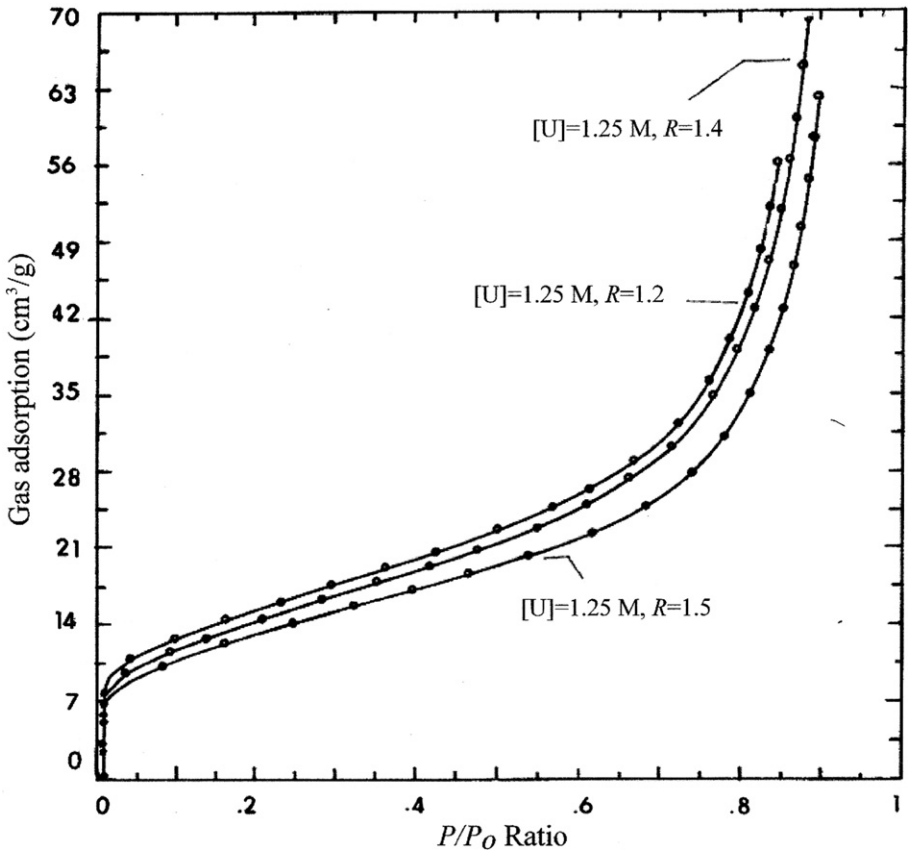

Fig. 2. Adsorption isotherms of N_2 for 250 °C heated (heating scheme A) microspheres.

the increase of metal ion concentration and decrease in R helps in decreasing the crush strength of the gel particles. They attributed this softness to the growth of large crystallites with the formation of gel network. In the present study with a fixed metal concentration and variable R, similar trend was also observed. Table 1 shows that for heating scheme A the crush strength decrease from 10.5 to 9.2 N/particle as the ratio R decreases from 1.5 to 1.2. The pore size distribution data depicted in Fig. 3 indirectly indicate increase in crystallite size with decrease in ratio R, confirming the observations of Pai et al. for thoria based systems. Suryanarayana et al. [13] reported similar observations for urania. They concluded that the higher metal ion concentration in the feed solution caused to lower the crush strength of the particles. But the softness of the particles prepared from the highest metal ion concentration which is practically achievable was still not adequate for the SGMP process. They suggested that an additional step of the calcination of UO_3 to U_3O_8, prior to its reduction to UO_2 imparts further softness to the particles. Under these circumstances the effect of calcination on softening the microspheres was examined as an important factor in this study.

3.2. Effect of heat treatment

As seen from Table 1, the dried microspheres (scheme A), the reduced microspheres (schemes B and C) and calcined microspheres (schemes D and E) did not show any noticeable trend in specific surface area, tap density and porosity with respect to feed composition variation. Further, it was also noticed that for a particular heating scheme the crush strength value increases with increase in R. But the minimum crush strength value of 4.8 N/particle obtained for feed composition [U] = 1.25 M and $R = 1.2$ heat treated by direct reduction of UO_3 microspheres to UO_2 microspheres (scheme B) was not soft enough for direct pelletization. This shows that by varying the feed composition alone it is not possible to obtain a product (UO_2) which is

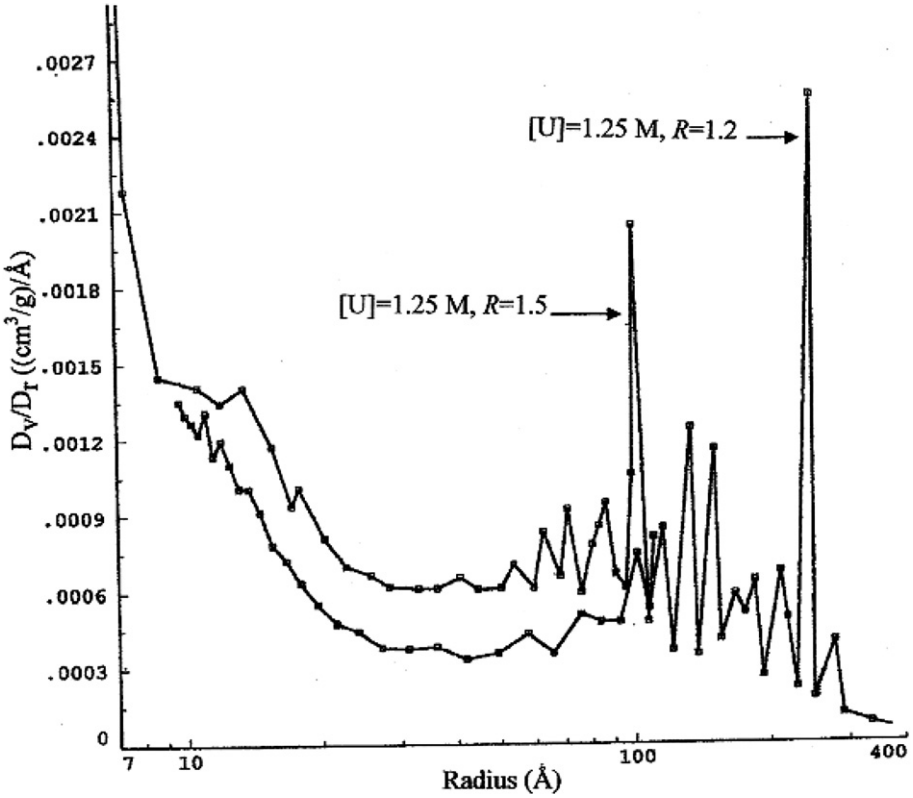

Fig. 3. Pore size distribution of 250 °C heated (heating scheme A) UO_3 microspheres.

suitable for pelletization by direct reduction of UO_3 microspheres to UO_2 microspheres. However, the table shows that there is a significant change in the properties of gel particles for a given feed composition when the heat treatment scheme was varied. It was also noticed that the lowest crush strength value for UO_2 microspheres (2.9 N/particle) was obtained when UO_3 microspheres were calcined to U_3O_8 and then reduced to UO_2 (scheme E) for the feed composition $[U] = 1.25$ and $R = 1.2$. These UO_2 microspheres are seen quite suitable for pelletization. Accordingly, further discussion is focused to the physical properties of the gel particles which were formed from the feed composition $[U] = 1.25$ M, $R = 1.2$ and heated under various heating conditions.

3.2.1. Gel particles dried at 250 °C

The adsorption–desorption isotherms of 250 °C dried (scheme A), directly reduced (scheme B) and calcined (scheme D) samples for the compositions $[U] = 1.25$ M, $R = 1.2$ are quite different as seen from Fig. 5. According to de Boer, the hysteresis loop in the adsorption–desorption curves (the lower curve in all the hysteresis loop is of adsorption isotherm and the upper curve is of desorption isotherm) of the 250 °C heated samples is of type B [24]. This type of hysteresis loop is associated with slit-shaped pores. The formation of slit-shaped pores in UO_3 may be caused from the hexagonal platelet shaped crystallites of hydrated UO_3 gel network [25]. SEM examination was carried out for intact microspheres (outer surface) and fractured microspheres (inner surface). Figs. 6(a) and 6(b) depict micrographs for intact and fractured dried UO_3 microspheres. This oxide is seen to be quite porous, and the outer and inner surfaces are of similar shape, although it is difficult to discuss by this magnification about the shape of the pores, which have the dimensions of Å order.

3.2.2. Directly reduced gel particles

For directly reduced UO_2 (heating scheme B), the adsorption–desorption isotherm hysteresis shown in Fig. 5 is of Type A [24], which indicates the presence of cylindrical pores. The pore size distribution pattern, shown in Fig. 4 (heating scheme B), are shifted on the higher side compared with those of Fig. 3 for

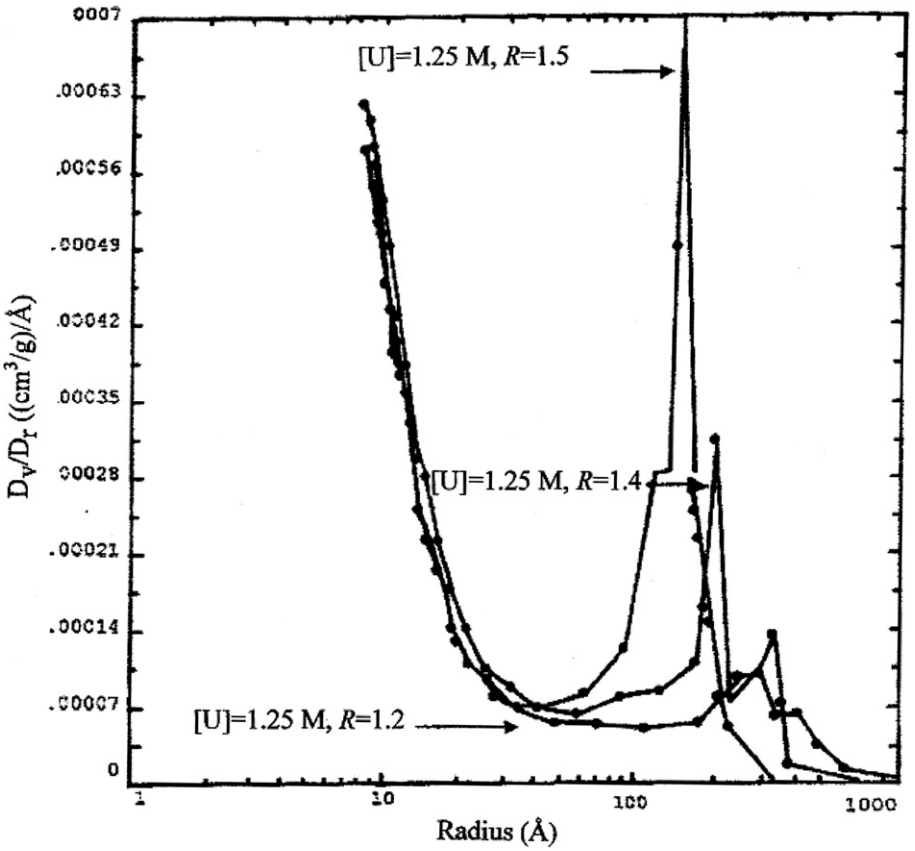

Fig. 4. Pore size distribution of the samples obtained by direct reduction at 600 °C (heating scheme B) of uranium oxides from different feed compositions.

250 °C heated sample (heating scheme A) because of product densification and pore coalescence. From the above observation and the physical properties listed in Table 2, it can be considered that the slit-shaped pores are transformed to cylindrical pores with moderate reduction in surface area and pore volume together with increase in pore size, when the UO_3 microsphere are directly reduced to UO_2 at 600 °C. This change could be attributed to the combined effect of the transformation from low-density phase (UO_3) to high-density phase (UO_2) and the growth of crystallites accompanied by coalescing (merging) of pores governed by reduction in surface energy of the system. The microstructure obtained for the product heated at 800 °C (scheme C) did not show any significant difference from those obtained for 600 °C (scheme B) heated product. As seen from Table 2, the tap density and the crush strength values are higher for particles reduced at higher temperature. The SEM photographs of the outer surface and the fractured (inner) surface of directly reduced (heating scheme C) UO_2 microspheres are shown in Figs. 7(a) and 7(b) respectively. These microstructures were observed to be similar to that of the microstructures of dried UO_3 microspheres (Figs. 6(a) and 6(b)) except for the prominence in pores due to increased dimensions. It is difficult to confirm whether the change of pore shape occurs from slit type to cylindrical type by this magnification.

3.2.3. Calcined gel particles

When the 250 °C heated samples were calcined at 800 °C in air (heating scheme D), the surface area and pore volume decreased to 6.75 m^2/g and 0.0055 cm^3/g, respectively (Table 2). The hysteresis loop shown in Fig. 5 is very small and resembles type C curve [24] which is associated with wedge shaped pores. This result shows that the slit-shaped pores collapsed into wedge shaped pores during decomposition of UO_3 to U_3O_8. The directly reduced samples (heating scheme B) indicate that

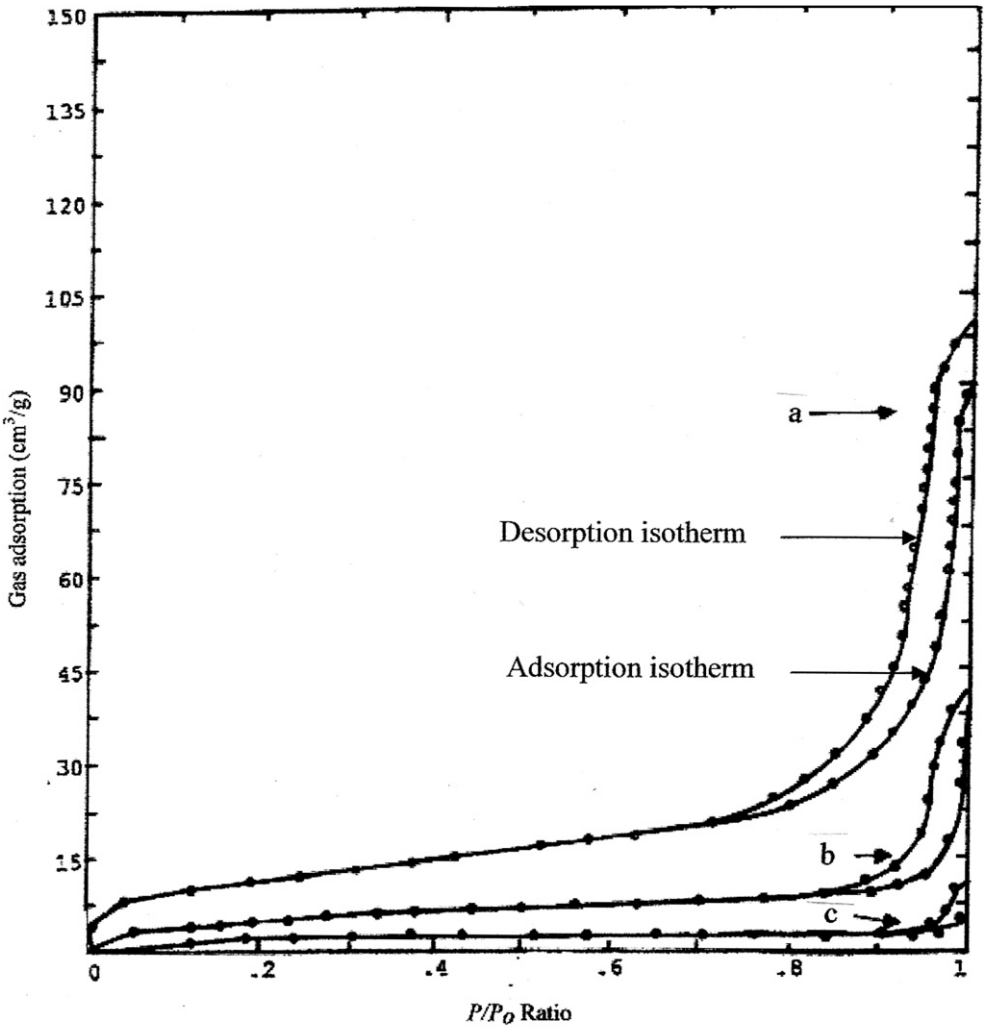

Fig. 5. Adsorption–desorption isotherm for N_2 for 250 °C heated (heating scheme A), directly reduced (heating scheme B) and calcined (heating scheme D) microspheres.

the change in tap density is not proportional to change in surface area and pore volume when compared with those of 800 °C calcined samples (heating scheme D). During the calcination of dried particles, the surface area is seen to be decreased as a result of collapse of pores with the retention of large number of closed pores in the calcined particle. The pore size distribution and cumulative specific pore volume curves for intact and fractured calcined particles shown in Fig. 8 clearly supports this explanation which is further confirmed by SEM investigation. The SEM micrographs of the outer surface and fractured surface (inner surface) of calcined microspheres are shown in Figs. 9(a) and 9(b), respectively. It can be seen from the micrographs that the outer surface of the particles is distinctly different from the inner surface. The porosity of the outer surface appears to be much lesser than that of the inner surface, confirming the results of the gas adsorption experiments. This could be explained on the basis of the mechanism of the decomposition reaction suggested by Bamankar et al. [26]. During calcination, UO_3 decomposes to U_3O_8 and O_2(g). The reaction initiates at the surface of the particles, and the reaction front then moves into the particles with the progress of the reaction.

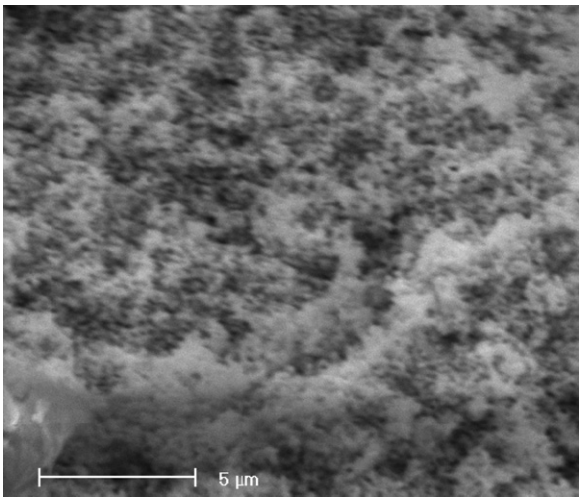

Fig. 6(a). SEM photograph of the outer surface of the 250 °C heated (heating scheme A) UO_3 microspheres.

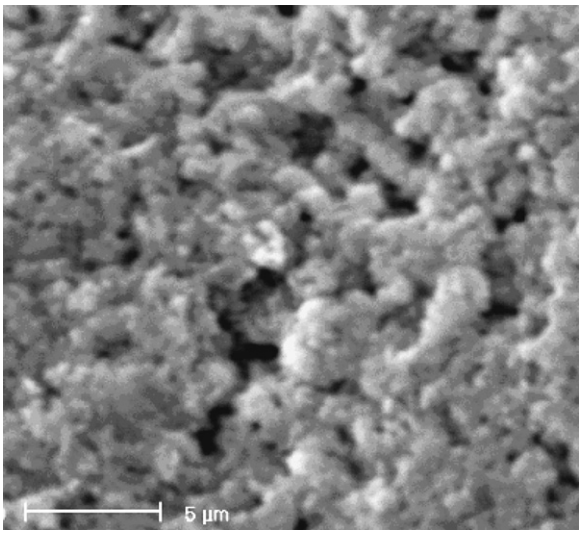

Fig. 6(b). SEM photograph of fractured (inner) surface of 250 °C heated (heating scheme A) UO_3 microspheres.

At the surface of the particles, release of O_2(g) occurs against the $P(O_2)$ of the gas phase over the solid, which is air in the present study. This reaction must result in collapse of the pores with transformation of their structures into wedge shaped shallow pores having larger diameters. This U_3O_8 product layer with low porosity (small surface area and pore volume listed in Table 1 and SEM photograph shown in Fig. 9(a)) hinders efficient release of product O_2(g), leading to build-up of oxygen pressure. Dell and Wheeler [27] reported this phenomenon as that to take place during the decomposition of 150 μm size UO_3 particles. They further reported that the higher reaction rate leads to cracking in the particles due to higher build-up of pressure. This pressure increase is supposed to be responsible for the inside porosity and some residual strain which ultimately imparts softness to the particles. The crush strength decreases from 9.2 to 0.8 N/particle as shown in Table 2.

3.2.4. Calcined and reduced gel particles

The pore size distribution curve for the sample of feed composition [U] = 1.25 M and $R = 1.2$ calcined in air at 800 °C for 1 h followed by reduction in 8%H_2/92%N_2 at 600 °C for 1 h (heating scheme E) is shown in Fig. 10, together with that for the sample without reduction process (heating scheme D). The morphology of the spheres remain essentially unchanged by the reduction treatment showing the same pore size distribution pattern. The hysteresis

Table 2
Physical properties of UO_3 microspheres heated under various heating conditions

No.	Heating scheme	Surface area (m^2/g)	Specific pore volume (cm^3/g)	Pore shape	Tap density (g/cm^3)	Crush strength (N/particle)
1	A	51.55	0.1079	Slit	1.52	9.2
2	B	17.26	0.0317	Cylindrical	2.39	4.8
3	C	15.68	0.0166	Cylindrical	2.54	6.3
4	D	6.75	0.0055	Wedge	1.62	0.8
5	E	6.46	0.0051	Wedge	2.13	2.9
6	F	18.87	0.0076	Cylindrical	–	–

Feed composition [U] = 1.25 M, $R = 1.2$.
A: UO_3 heated in air at 250 °C for 4 h.
B: Direct reduction of UO_3 to UO_2 in 8%H_2/92%N_2 gas at 600 °C for 1 h.
C: Direct reduction of UO_3 to UO_2 in 8%H_2/92%N_2 gas at 800 °C for 1 h.
D: Calcination of UO_3 to convert to U_3O_8 in air at 800 °C for 1 h.
E: Calcination of UO_3 to convert to U_3O_8 in air at 800 °C for 1 h followed by reduction to UO_2 in 8%H_2/92%N_2 gas at 600 °C for 1 h.
F: Fragmented microspheres from the heating scheme D.

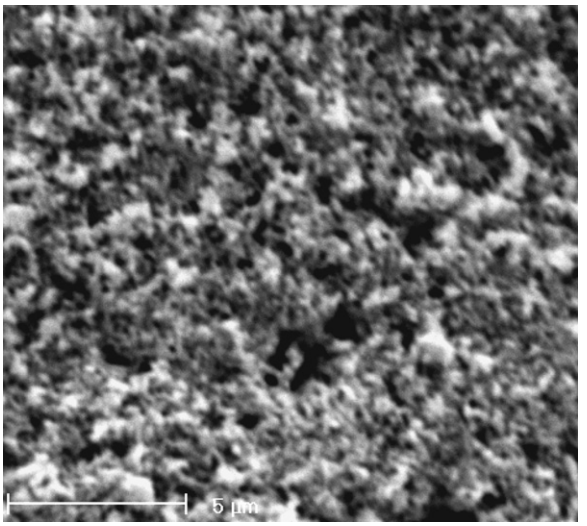

Fig. 7(a). SEM photograph of outer surface of directly reduced (heating scheme C) UO_2 microspheres.

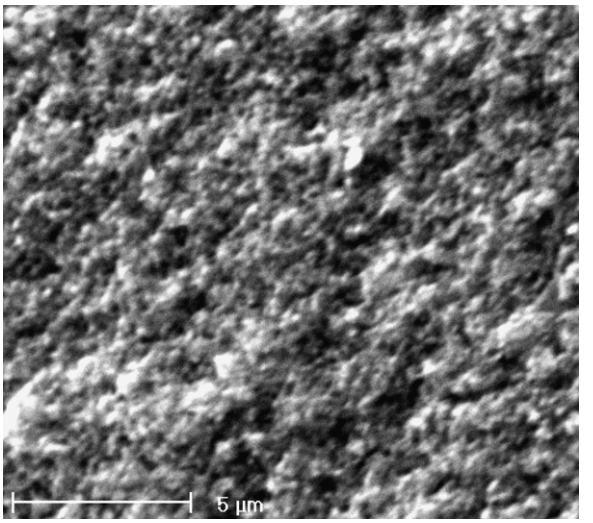

Fig. 7(b). SEM photograph of fractured (inner) surface of directly reduced (heating scheme C) UO_2 microspheres.

pattern of the calcined and reduced sample (not shown in Fig. 5) was also similar to that of the calcined sample indicating that the shape of the pore also remained unchanged. From Table 2 it is seen that there is no large change in the surface area and pore volume but the crush strength and tap density increase. The crush strength values are, however, still within the acceptable value

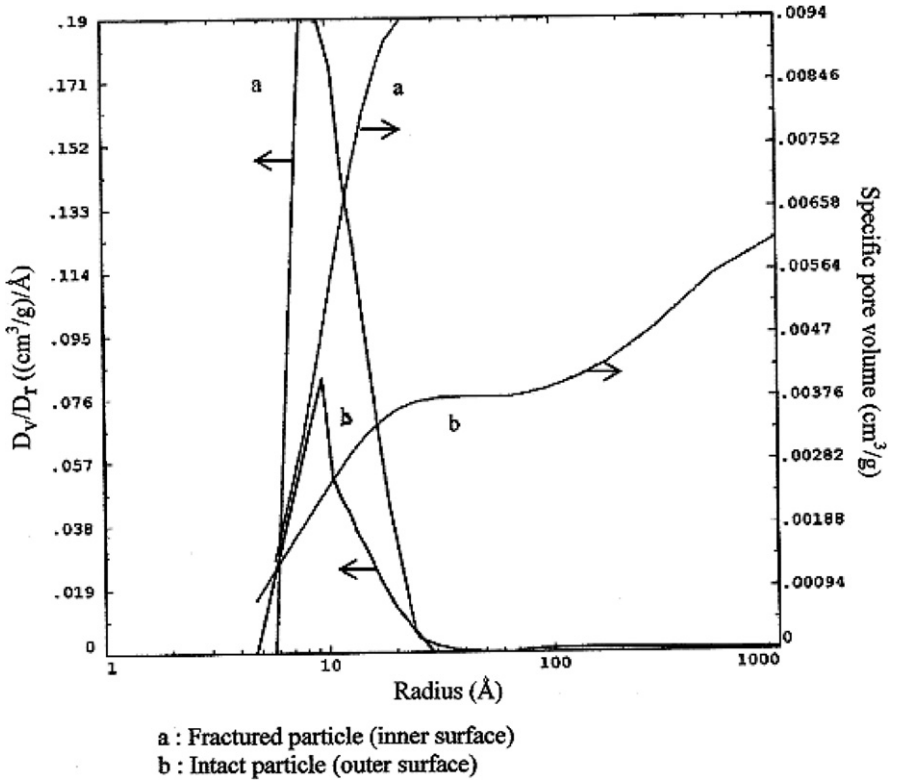

Fig. 8. Pore-size distribution of calcined (heating scheme D) intact U_3O_8 microspheres together with calcined (heating scheme D) and fractured U_3O_8 microspheres.

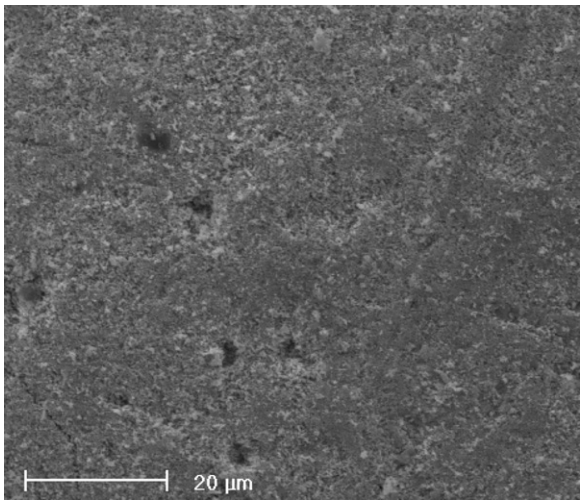

Fig. 9(a). SEM photograph of outer surface of calcined (heating scheme D) U_3O_8 microspheres.

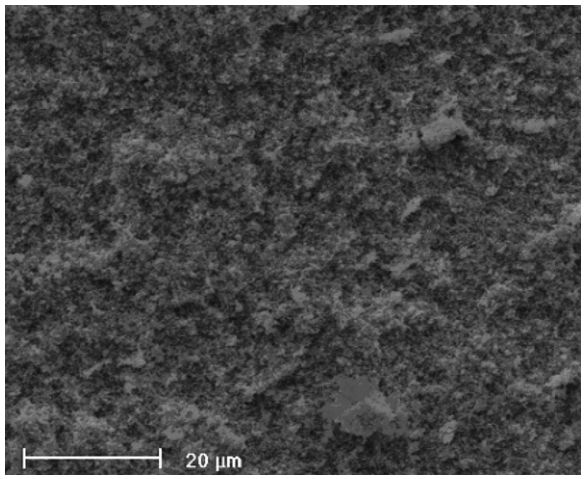

Fig. 9(b). SEM photograph of fractured (inner) surface of calcined (heating scheme D) U_3O_8 microspheres.

(2–3 N/particle) for having the pellets of good quality reported by Suryanarayana et al. [13]. The microstructure of the calcined particles was retained when they were reduced to UO_2 by hydrogen as shown in

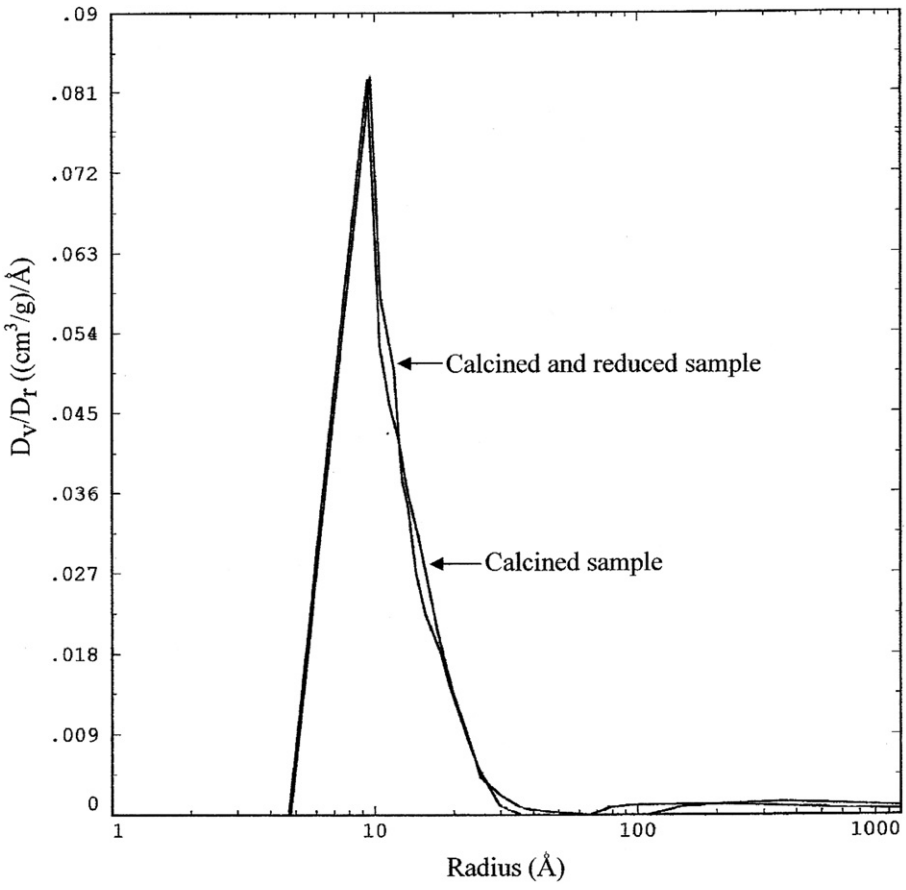

Fig. 10. Pore size distribution curve for calcined (heating scheme D) U_3O_8 and calcined and subsequently reduced (heating scheme E) UO_2 microspheres.

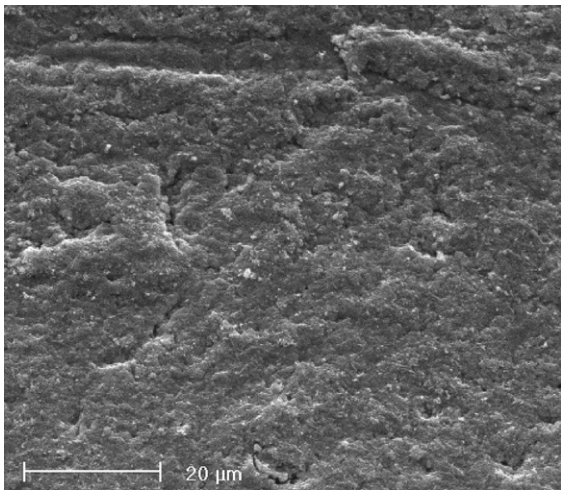

Fig. 11(a). SEM photograph of outer surface of calcined and reduced (heating scheme E) UO_2 microspheres.

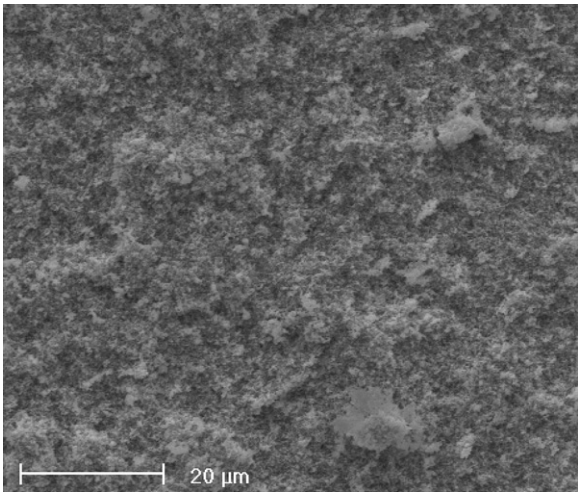

Fig. 11(b). SEM photograph of fractured (inner) surface of calcined and reduced (heating scheme E) UO_2 microspheres.

Figs. 11(a) and 11(b). These closed pores in the UO_2 product give softness in the particles which is very important for their pelletization into high quality pellets.

4. Conclusion

Both the composition of the feed solution and the heat treatment condition, have significant effect on the morphology of the resulting product. The composition of the feed solution has considerable effect on the pore size and crush strength of directly reduced UO_2 microspheres. The pore size decreases and the crush strength increases with the increase in [HMTA-urea]/[U] mole ratio, R, for a given metal ion concentration. Heat treatment experiments showed that 250 °C heated spheres have slit type pores which on calcination are converted to wedge type pores with substantial decrease in the surface area and pore volume. Namely, collapse occurs in the structure during the process forming many closed pores which result in formation of soft product particles. This conclusion is well supported by the SEM photographs of the calcined spheres, which clearly show the presence of fewer pores on the outer surface and that of plenty of pores on the fractured inner surface. In the case of directly reduced spheres, such a wide variation is not observed in the porosity distribution. The minimum crush strength for the microspheres prepared from feed composition of [U]=1.25 M and $R = 1.2$ was 4.8 N/particle for directly reduced samples. However, these particles are not soft enough for SGMP. Subsequent reduction after calcination yields softer product (crush strength 2.9 N/particle) than the product obtained by direct reduction. It can be concluded that the calcination alters the morphology of the resulting UO_2 product in such a way that it imparts softness to the particles making them suitable for direct pelletization.

Acknowledgements

The authors thank Dr S.K. Aggarwal, Head, Fuel Chemistry Division for his support and encouragement during the course of the investigation. The authors also express their sincere thanks to Mr D.N. Sah, Head, Post Irradiation Examination Division, for the SEM examinations.

References

[1] J.B.W. Kanj, A.J. Noothout, O. Votocik, IAEA-161, 1974, p. 185.
[2] V.N. Vaidya, S.K. Mukerjee, J.K. Joshi, R.V. Kamat, D.D. Sood, J. Nucl. Mater. 148 (1987) 324.
[3] R.B. Mathews, P.E. Hart, J. Nucl. Mater. 92 (1980) 207.
[4] S.M. Tiegs, P.A. Haas, R.D. Spence, Oak Ridge National Laboratory Report, ORNL/TM-6906, 1979.
[5] P.A. Hass, J.M. Begovich, A.D. Ryon, J.S. Vavruska, Oak Ridge National Laboratory Report, ORNL/TM-6850, 1979.
[6] A.L. Lotts (compiler), USAEC report, ORNL-4901, 1973.
[7] E. Zimmer, C. Ganguly, J. Borchaedt, H. Langen, J. Nucl. Mater. 152 (1988) 169.
[8] C. Ganguly, J. Basak, V.N. Vaidya, D.D. Sood, P.R. Roy, Proc, of 2nd Conf. on CANDU Fuel, Perbroke, October 1–5, 1989, p. 104.

[9] C. Ganguly, H. Langan, E. Zimmer, E. Merz, Nucl. Technol. 73 (1986) 84.
[10] C. Ganguly, U. Basak, J. Nucl. Mater. 178 (1991) 179.
[11] C. Ganguly, E. Zimmer, Merz, Trans. Am. Nucl. Soc. 52 (1986) 44.
[12] C. Ganguly, Metals Mater. Process. 1 (1980) 253.
[13] S. Suryanarayana, N. Kumar, Y.R. Bamankar, V.N. Vaidya, D.D. Sood, J. Nucl. Mater. 230 (1996) 140.
[14] R. Forthmann, H. Nickel, A. Naomidis, W. Burck, Jul-655-RW-KFA-Julich Report, 1970.
[15] R. Forthmann, G. Blass, J. Nucl. Mater. 64 (1977) 275.
[16] S. Brunauer, P. Emmett, E. Teller, J. Am. Chem. Soc. 60 (1938) 309.
[17] W.T. Thomson, Philos. Mag. 42 (1871) 448.
[18] E.P. Barrett, L.G. Joyner, P.P. Halenda, J. Am. Chem. Soc. 73 (1951) 373.
[19] G. Horvath, K. Kawazoe, J. Chem. Eng. 166 (1983) 470.
[20] N. Kumar, Y.R. Bamankar, K.T. Pillai, S.K. Mukerjee, V.N. Vaidya, V. Venugopal, Indian Nuclear Society Annual Conference (INSAC 2003), IGCAR, Chennai, India, 2003, A-16.
[21] S. Brunaeur, L.S. Deming, W.S. Deming, E. Teller, J. Am. Chem. Soc. 62 (1940) 1723.
[22] J.L. Collins, M.H. Lloyd, R.L. Fellows, Radiochim. Acta 42 (1987) 121.
[23] Rajesh V Pai, S.K. Mukerjee, V.N. Vaidya, J. Nucl. Mater. 325 (2004) 159.
[24] J.H. de Boer, The Structure and Properties of Porous Materials, Butterworth, London, 1958, p. 68.
[25] M.H. Lloyd, K. Bischoff, K. Peng, H.U. Nissen, R. Wessicken, J. Inorg. Nucl. Chem. 38 (1976) 114.
[26] Y.R. Bamankar, N. Kumar, K.T. Pillai, S.K. Mukerjee, V.N. Vaidya, Nuclear and Radiochemistry Symposium, NUCAR 2005, Amritsar, India, 2005, p. 269.
[27] R.M. Dell, V.J. Wheeler, Trans. Faraday Soc. 58 (1962) 485.